

Performance analysis for a chaos-based code-division multiple access system in wide-band channel

Ciprian Doru Giurcăneanu¹, Raneetha Vasundara Abeywickrama¹, Stevan Berber²

¹Department of Statistics, University of Auckland, Auckland, New Zealand

²Department of Electrical and Computer Engineering, University of Auckland, Auckland, New Zealand

E-mail: c.giurcaneanu@auckland.ac.nz

Published in *The Journal of Engineering*; Received on 29th June 2015; Accepted on 13th July 2015

Abstract: Code-division multiple access technology is widely used in telecommunications and its performance has been extensively investigated in the past. Theoretical results for the case of wide-band transmission channel were not available until recently. The novel formulae which have been published in 2014 can have an important impact on the future of wireless multiuser communications, but limitations come from the Gaussian approximations used in their derivation. In this Letter, the authors obtain more accurate expressions of the bit error rate (BER) for the case when the model of the wide-band channel is two-ray, with Rayleigh fading. In the authors' approach, the spreading sequences are assumed to be generated by logistic map given by Chebyshev polynomial function of order two. Their theoretical and experimental results show clearly that the previous results on BER, which rely on the crude Gaussian approximation, are over-pessimistic.

1 Introduction and preliminaries

In CDMA (code-division multiple access) systems, each bit is transmitted by using a sequence of chips, $x_1, x_2, \dots, x_{2\beta}$, where 2β is called spreading factor. We prefer to use the vector notation, $\mathbf{x} = [x_1, x_2, \dots, x_{2\beta}]^T$, where the operator $(\cdot)^T$ denotes the transposition. In the case of chaos-shift-keying-based CDMA systems [1–3], a chaotic map, say $g(\cdot)$, is employed to generate \mathbf{x} as follows: x_1 is randomly drawn from the natural invariant distribution of the map and $x_{i+1} = g(x_i)$ for $i \in \{1, 2, \dots, 2\beta - 1\}$. For example, if the logistic map given by Chebyshev polynomial function of order two is employed, then $x_{i+1} = 1 - 2x_i^2$ [4]. According to the bit value ('+1' or '-1'), the transmitter sends either \mathbf{x} or $-\mathbf{x}$. At the receiver site, the incoming signal is not exactly the same as the one which was transmitted because is affected by fading, white Gaussian noise is added and other chaotic sequences are superposed. These sequences represent bits sent to other users and they are generated by applying the same method as above, except that their first entry is chosen to be statistically independent from x_1 . The receiver correlates the received signal with a locally generated copy of \mathbf{x} and the result is further compared with a threshold in order to decide if the received bit is either '+1' or '-1'. The bit error rate (BER) is given by the number of erroneously decoded bits in respect to the total number of bits received [5, 6].

In recent years, novel chaos-based CDMA systems have been introduced, some of which are differential chaos-shift keying systems. Articles presenting this type of research can be found either in telecommunications journals [6, 7], or in publications of the researchers working in the field of circuits and systems [8–11]. We do not plan to discuss here the content of these works. However, it is important to observe that the inventors of the new systems provide theoretical and experimental evaluations of BER, in order to show the superiority in comparison with the already existing CDMA systems. In what concerns theoretical analysis, there are two important methodologies. The first one relies on a Gaussian approximation which is known to be accurate when the spreading factor is high. The origins of this approach can be traced back to [12, 13]. The methods from the second class use a special type of numerical integration which was introduced in [14] and since then was successfully applied for BER estimation when the spreading factor is low. A possible alternative is the method from [5], but it is rarely used because is computationally

intensive. A more detailed comparison of these methods can be found, for example, in [15]. Other techniques can be found in [16, 17].

The scenario we have discussed so far corresponds to the case of a narrow-band channel. For the wide-band channel [1], the Saleh–Valenzuela model [18, 19] is adopted. Each entry of the chaotic sequence is repeated s times such that the new sequence is

$$\underbrace{x_1, \dots, x_1}_{s \text{ samples}}, \underbrace{x_2, \dots, x_2}_{s \text{ samples}}, \dots, \underbrace{x_{2\beta}, \dots, x_{2\beta}}_{s \text{ samples}}$$

The receiver gets messages not only through the main path, but also through the secondary paths. More importantly, the delay on each secondary path is different from the delay on the main path. Therefore, the structure of the received signal is much more complicated because it contains multiple delayed copies of the original message. Like in the case of narrow-band channel, the receiver correlates this signal with the chaotic sequence of the user and produces the output z , which is further compared with a threshold in order to decide if the received bit is either '+1' or '-1'. Obviously, z is a random variable because of the randomness of the chaotic sequences as well as the randomness of fading, delay and additive noise on each path from the transmitter to the receiver. The very first theoretical BER formula for wide-band channel was recently derived, under the assumption that z is Gaussian distributed [1]. However, there exists empirical evidence that this crude approximation leads to over-pessimistic results in the case when the number of secondary paths is small.

In this work, we propose to compute BER with higher accuracy. We focus on the case when the chaotic sequences are generated by using logistic map and assume that there are two propagation paths from the transmitter to the receiver. Both paths experience Rayleigh fading and are affected by additive white Gaussian noise. The secondary path is delayed in time by τ , which represents a portion of the chip interval. With the aforementioned convention that each chip is extended into s samples, we have $0 \leq \tau \leq s$. We refer to [1] for more details about this model. The main contributions of this Letter are the following:

- In Section 3, we compute the BER conditional on random variables which model fading and delay, and then apply the law of total

probability for continuous distributions [20]. In addition, we pay a special attention to the probabilistic model of delays, which are non-negative integers, because the simplified models that have been used in the previous literature treated them as *continuous* random variables. Since we are interested in evaluating the influence of the secondary path and that of the additive Gaussian noise, we compute the theoretical BER for four different cases.

- For a fair comparison, in Section 4, we apply the crude Gaussian approximation from [1] in order to evaluate the approximate BER's in the four cases we analyse.
- In Section 5, we resort to numerical examples for demonstrating that our formulae for BER are more precise than those given by the crude Gaussian approximation. A discussion on the theoretical and empirical results of this Letter can be found in Section 6.

Owing to the limited typographic space, we cannot outline below all the results we have obtained. This is why we present in this Letter only the most important results, and the interested reader can find more details in the supplemental material [21]. In the following section, we provide a more formal description of the system which is studied in this work.

2 System model

Our main concern is the random variable z . Before giving its expression as it appears in [1], we introduce some definitions.

Assume that the received signal is the superposition of the messages from N users. Let the chaotic sequence for the n th user be $\mathbf{x}^{(n)} = [x_1^{(n)}, x_2^{(n)}, \dots, x_{2\beta}^{(n)}]^\top$. Without loss of generality, we assume that chaotic sequence of the user who received the signal is $\mathbf{x}^{(1)}$, and define

$$a_n = (\mathbf{x}^{(n)})^\top \mathbf{x}^{(1)} = (\mathbf{x}^{(1)})^\top \mathbf{x}^{(n)}. \quad (1)$$

Furthermore, we denote $A = a_1 + a_2 + \dots + a_N$. For writing the equations more compactly, we also introduce

$$\mathbf{x}_d^{(n)} = [x_0^{(n)}, x_1^{(n)}, \dots, x_{2\beta-1}^{(n)}]^\top, \quad \text{for all } n \in \{1, 2, \dots, N\}.$$

In the equation above, we use the convention that $x_0^{(n)} = x_{2\beta}^{(n)}$. In addition, we define

$$b_n = (\mathbf{x}_d^{(n)})^\top \mathbf{x}^{(1)} = (\mathbf{x}^{(1)})^\top \mathbf{x}_d^{(n)} \quad (2)$$

and $B = b_1 + b_2 + \dots + b_N$. For modelling the additive noise, we

consider the zero-mean Gaussian random vector

$$\xi = [\xi_1, \xi_2, \dots, \xi_{2\beta}]^\top, \quad (3)$$

whose covariance matrix equals $N_0 \mathbf{I}$, where $N_0 > 0$ and \mathbf{I} denotes the identity matrix of appropriate dimension. Let $C = \xi^\top \mathbf{x}^{(1)}$. The entries of ξ and those of $\mathbf{x}^{(n)}$, $\mathbf{x}_d^{(n)}$ are statistically independent for all $n \in \{1, 2, \dots, N\}$.

The random variable z , which is used to decide if value of the received bit is either '+1' or '-1', is computed as the correlation between the received signal and the locally generated sequence $\mathbf{x}^{(1)}$. The contribution to the received signal of the n th user ($1 \leq n \leq N$) is described in Table 1. Using the results from the table, it is straightforward to write down the expression of z [1]

$$z = \delta_0 A + \delta_1 \tau B + sC, \quad (4)$$

with the convention that

$$\delta_0 = \alpha_{00}s + \alpha_{01}(s - \tau), \quad (5)$$

$$\delta_1 = \alpha_{01}\tau. \quad (6)$$

In our derivations, we use the following assumptions:

(A₁) The chaotic sequence for each user is generated by using the logistic map (see Section 1). The very first entry of each such chaotic sequence is drawn from the distribution given in [4, Eq. (7)] such that, for any two different users, the very first entries of their chaotic sequences are statistically independent.

(A₂) The main path and the secondary path (where the delay τ occurs) are affected by Rayleigh fading (see Table 1). The fading factor remains constant over a transmitted bit interval [1]. The parameter of the Rayleigh distribution used to model the fading on the main path is denoted b . For the secondary path, the parameter is \tilde{b} . So, we write $\alpha_{00} \sim \text{Rayleigh}(b)$ and $\alpha_{01} \sim \text{Rayleigh}(\tilde{b})$. We emphasise that α_{00} and α_{01} are statistically independent. In our calculations, the following results are useful [22, Chapter 35]

$$E[\alpha_{00}] = b\left(\frac{\pi}{2}\right)^{1/2}, \quad (7)$$

$$E[\alpha_{00}^2] = 2b^2, \quad (8)$$

where $E(\cdot)$ denotes the expectation operator. The moments of α_{01} can be obtained by replacing b with \tilde{b} in the expressions above.

(A₃) For $n \in \{1, 2, \dots, N\}$, the random variables α_{00} and α_{01} are statistically independent in rapport with the entries of the vectors $\mathbf{x}^{(n)}$, $\mathbf{x}_d^{(n)}$ and ξ .

Table 1 Contribution of the n th user to the received signal: α_{00} and α_{01} are statistically independent Rayleigh random variables which model the fading for the main path and the secondary path, respectively. In comparison with the main path, the secondary path is delayed in time by τ . The design parameter s plays a key role as each chip is extended into s samples in order to analyse the performance of the system when the secondary path is delayed by only a portion of the chip interval. It is obvious that $0 \leq \tau \leq s$. To be in line with the analysis from [1], we assume that the 'true' value of the received bit is '+1' and the 'true' value of the previous bit is also '+1'

Path	Fading	Chip		
		1	...	2β
main	α_{00}	$\underbrace{x_1^{(n)} \dots x_1^{(n)}}_{s \text{ samples}}$...	$\underbrace{x_{2\beta}^{(n)} \dots x_{2\beta}^{(n)}}_{s \text{ samples}}$
secondary	α_{01}	$\underbrace{x_{2\beta}^{(n)} \dots x_{2\beta}^{(n)}}_{\tau \text{ samples}} \underbrace{x_1^{(n)} \dots x_1^{(n)}}_{s-\tau \text{ samples}}$...	$\underbrace{x_{2\beta-1}^{(n)} \dots x_{2\beta-1}^{(n)}}_{\tau \text{ samples}} \underbrace{x_{2\beta}^{(n)} \dots x_{2\beta}^{(n)}}_{s-\tau \text{ samples}}$

3 Theoretical BER

3.1 Main idea

The analysis from [21], which is based on computing the skewness [23, Eq. (3.89)] for each term within (4), suggests that the Gaussian assumption for z is inappropriate in the case when the number of secondary paths is small. However, from the same analysis we know that, for large β , the Gaussian distribution might be a good approximation for the conditional distribution of z given α_{00} , α_{01} and τ (see also [13, 24]). This leads to the natural choice of computing first the conditional BER and then applies the law of total probability (for continuous distributions). This approach is in line with what has been already done for similar problems, in the case of narrow-band channels (see, e.g. [20]). The details of the calculations are outlined below.

3.2 Conditional BER

Given α_{00} , α_{01} , τ and the fact that the 'true' value of the transmitted bit is '+1', BER is obtained by computing $\Pr(z < 0 | \alpha_{00}, \alpha_{01}, \tau)$. Therefore, we have

$$\begin{aligned} \text{BER}(\alpha_{00}, \alpha_{01}, \tau) &= \frac{1}{2} \text{erfc} \left(\frac{E[z | \alpha_{00}, \alpha_{01}, \tau]}{\sqrt{2 \text{Var}[z | \alpha_{00}, \alpha_{01}, \tau]}} \right) \\ &= \frac{1}{2} \text{erfc} \left(\left\{ \frac{2 \text{Var}[z | \alpha_{00}, \alpha_{01}, \tau]}{(E[z | \alpha_{00}, \alpha_{01}, \tau])^2} \right\}^{-1/2} \right), \end{aligned} \quad (9)$$

where $\text{erfc}(\cdot)$ has the well-known expression [2, p. 48]

$$\text{erfc}(\psi) = \frac{2}{\sqrt{\pi}} \int_{\psi}^{\infty} \exp(-\omega^2) d\omega.$$

Next, we employ results which are proved in [21, Chapter 3] (see Lemma 3.2.2, Lemma 3.2.4 and Lemma 3.3.1) in order to calculate

$$\begin{aligned} E[z | \alpha_{00}, \alpha_{01}, \tau] &= \delta_0 E[A] + \delta_1 E[B] + sE[C] = \frac{\delta_0}{2} (2\beta), \\ E[z^2 | \alpha_{00}, \alpha_{01}, \tau] &= \delta_0^2 E[A^2] + \delta_1^2 E[B^2] + s^2 E[C^2] + 2\delta_0 \delta_1 E[AB] \\ &= \delta_0^2 \left[\frac{N}{4} (2\beta) + \frac{1}{4} (2\beta)^2 - \frac{1}{8} (2\beta) \right] \\ &\quad + \delta_1^2 \frac{N}{4} (2\beta) + s^2 \frac{N_0}{2} (2\beta) + 2\delta_0 \delta_1 \frac{1}{8} (2\beta - 2), \end{aligned}$$

where δ_0 and δ_1 are given in (5) and (6), respectively.

The quantity of interest for us is

$$\frac{2 \text{Var}[z | \alpha_{00}, \alpha_{01}, \tau]}{(E[z | \alpha_{00}, \alpha_{01}, \tau])^2} = \left(\frac{\delta_1}{\delta_0} \right)^2 \frac{2N}{2\beta} + \left(\frac{\delta_1}{\delta_0} \right) \frac{2(2\beta - 2)}{(2\beta)^2} \quad (10)$$

$$+ \left(\frac{1}{\delta_0} \right)^2 N_0 \frac{4s^2}{2\beta} \quad (11)$$

$$+ \frac{2N - 1}{2\beta}. \quad (12)$$

Under the hypothesis that $\alpha_{01} \neq 0$, $\tau \neq 0$ and $r = \alpha_{00}/\alpha_{01}$, we can rearrange some of the terms in the equation above

$$\frac{\delta_1}{\delta_0} = \frac{1}{(s/\tau)(r+1) - 1}, \quad (13)$$

$$\left(\frac{1}{\delta_0} \right)^2 N_0 \frac{4s^2}{2\beta} = \frac{N_0}{\beta \alpha_{00}^2} \frac{2}{[1 + (1/r)(1 - (\tau/s))]^2}. \quad (14)$$

These identities lead to the following conclusions:

- Remark in (14) that the term $N_0(\beta \alpha_{00}^2)^{-1}$ can be written as $N_0(E_b \alpha_{00}^2)^{-1}$, where E_b is the bit energy and equals $2\beta E[x_i^2]$. We refer to [20, Eq. (14)] for the definition of the bit energy. The reader can also see in [21, Eq. (3.5)] that $E[x_i^2] = 1/2$ for the logistic map. Combining the results from (9), (11) and (14), we can conclude that the BER decreases when the product $E_b \alpha_{00}^2$ raises. It is also interesting to note that the positive factor which multiplies $N_0(\beta \alpha_{00}^2)^{-1}$ in (14) is smaller than two for all possible values of r , τ and s .

- The performance is the same for all selections of s and τ for which the ratio s/τ has a certain value. An increase of s/τ guarantees a lower BER [see again (9), (10) and (14)].

- The increase of r has mixed effects in the sense that δ_1/δ_0 decreases, whereas the value of the expression in (14) grows.

3.3 Average BER

To gain more insight, we investigate separately the influence of the second propagation path and that of the additive Gaussian noise. Then we treat the general case.

Case #1: Effect of additive noise is neglected ($N_0 = 0$). If we ignore the term in (11), then $E_b/N_0 = \infty$ and the expression of conditional BER becomes

$$\text{BER}(r, \tau) |_{E_b/N_0 = \infty} = \frac{1}{2} \text{erfc}(\zeta_{r,\tau}^{-1/2}),$$

where

$$\zeta_{r,\tau} = \frac{N/\beta}{[(s/\tau)(r+1) - 1]^2} + \frac{(\beta-1)/\beta^2}{(s/\tau)(r+1) - 1} + \frac{2N-1}{2\beta}.$$

Furthermore, we can calculate

$$\text{BER}(\tau) |_{E_b/N_0 = \infty} = \int_0^{\infty} [\text{BER}(r, \tau) |_{E_b/N_0 = \infty}] f(r) dr, \quad (15)$$

where $f(r)$ denotes the probability density function (PDF) of r . It follows from (A₂) that

$$f(r) = \frac{2rb^2\tilde{b}^2}{(r^2\tilde{b}^2 + b^2)^2}, \quad 0 < r < \infty$$

[25, Corollary 3.4].

Case #2: $N_0 > 0$, α_{00} and α_{01} are linearly dependent. Now we consider that

$$\alpha_{00}/\alpha_{01} = r_0, \quad (16)$$

where r_0 is fixed ($r_0 \geq 1$). This is a major deviation from (A₂), but it will help us to gain more insight on the problem we analyse: it is the case when the attenuation in the secondary path is higher than in the primary path, which is the expected behaviour of the practical channels. This assumption leads to

$$\text{BER}(\alpha_{00}, \tau) |_{r=r_0} = \frac{1}{2} \text{erfc}(\zeta_{\alpha_{00},\tau}^{-1/2}),$$

where

$$\begin{aligned}\zeta_{\alpha_{00},\tau} &= \frac{N}{D_1^2\beta} + \frac{\beta-1}{D_1\beta^2} + \frac{2N_0}{\alpha_{00}^2\beta D_2^2} + \frac{2N-1}{2\beta}, \\ D_1 &= \frac{\delta_0}{\delta_1} = \frac{s}{\tau}(r_0+1) - 1, \\ D_2 &= \frac{\delta_0}{\alpha_{00}s} = 1 + \frac{1}{r_0}\left(1 - \frac{\tau}{s}\right).\end{aligned}\quad (17)$$

We have

$$\text{BER}(\tau)|_{r=r_0} = \int_0^\infty [\text{BER}(\alpha_{00}, \tau)|_{r=r_0}] f(\alpha_{00}) d\alpha_{00}, \quad (18)$$

where

$$f(\alpha_{00}) = (\alpha_{00}/b^2) \exp[-\alpha_{00}^2/(2b^2)], \quad 0 < \alpha_{00} < \infty, \quad (19)$$

because $\alpha_{00} \sim \text{Rayleigh}(b)$ [see (A₂)]. For writing the formula in (18) in a more convenient form, we firstly re-write $\zeta_{\alpha_{00},\tau}$ as $\zeta_{\gamma,\tau}$

$$\zeta_{\gamma,\tau} = v + \frac{w}{\gamma}, \quad (20)$$

$$v = \frac{N}{D_1^2\beta} + \frac{\beta-1}{D_1\beta^2} + \frac{2N-1}{2\beta}, \quad (21)$$

$$w = \frac{2N_0}{\beta D_2^2}. \quad (22)$$

After some algebra, we get that the PDF of γ is $f(\gamma) = \exp(-\gamma/\bar{\gamma})/\bar{\gamma}$, where $0 < \gamma < \infty$ and $\bar{\gamma} = 2b^2$. So

$$\begin{aligned}\text{BER}(\tau)|_{r=r_0} &= \int_0^\infty [\text{BER}(\gamma, \tau)|_{r=r_0}] f(\gamma) d\gamma \\ &= \frac{1}{2} \int_0^\infty \text{erfc}(\zeta_{\gamma,\tau}^{1/2}) f(\gamma) d\gamma \\ &= \int_0^\infty Q(\sqrt{2}\zeta_{\gamma,\tau}^{1/2}) f(\gamma) d\gamma\end{aligned}\quad (23)$$

$$= \frac{1}{\pi} \int_0^\infty \left[\int_0^{\pi/2} \exp\left(-\frac{\zeta_{\gamma,\tau}}{\sin^2\theta}\right) d\theta \right] f(\gamma) d\gamma. \quad (24)$$

In (23), we have used the well-known relationship between the $\text{erfc}(\cdot)$ and the Gaussian Q -function. The reader can find more details in [26, p. 85], where is also presented the identity we employed in (24). The double integral in (24) cannot be easily computed, but it allows us to obtain a lower bound for $\text{BER}(\tau)|_{r=r_0}$.

Proposition 1: The following inequality holds true:

$$\text{BER}(\tau)|_{r=r_0} \geq \frac{1}{2} \left(1 - \frac{1}{\sqrt{1+w/\bar{\gamma}}} \right). \quad (25)$$

The proof is deferred to the Appendix.

Remarks:

- (i) From (22), we know that $w = (E_b/N_0)^{-1} \times (2/D_2^2)$. This shows clearly that the lower bound decreases when E_b/N_0 raises. The same identity shows that the lower bound also depends on r_0 , τ and s [see again the definition in (17)].

- (ii) The lower bound does not depend on the number of users N because, in the derivation of (25), the v -term from (20) was ignored. For example, if we take $N=4$ or $N=40$, the lower bound in (25) is the same (given that all other settings are the same). For illustration, we plot in Fig. 1 the values of the lower bound when $\beta = 50$, $r_0 = 1.1$, $s = 40$, $\tau \in \{1, 20, 39\}$ and $E_b/N_0 \in \{1 \text{ dB}, 2 \text{ dB}, \dots, 16 \text{ dB}\}$. In the same figure, we show the values of the integral in (18), which are numerically computed for $N=4$ and $N=40$, respectively. Note that the lower bound is a good approximation of the integral when $N=4$. It is not surprising that the approximation becomes much worse when N is large. This suggests that the lower bound might be used to approximate (18) only when N is small.

Case #3: $N_0 > 0$, α_{00} and α_{01} are statistically independent. With the convention that $\zeta_{\alpha_{00},\alpha_{01},\tau}$ is given by the expression in (10)–(12), we get

$$\text{BER}(\alpha_{00}, \alpha_{01}, \tau) = \frac{1}{2} \text{erfc}\left(\zeta_{\alpha_{00},\alpha_{01},\tau}^{-1/2}\right), \quad (26)$$

$$\text{BER}(\tau) = \int_0^\infty \int_0^\infty \text{BER}(\alpha_{00}, \alpha_{01}, \tau) f(\alpha_{00}) f(\alpha_{01}) d\alpha_{00} d\alpha_{01}, \quad (27)$$

where $f(\alpha_{00})$ is the same as in (19). We have from (A₂) that $f(\alpha_{01}) = (\alpha_{01}/\tilde{b}^2) \exp[-\alpha_{01}^2/(2\tilde{b}^2)]$, where $0 < \alpha_{01} < \infty$. For the evaluation of the integral in (27) can be used, e.g. the Matlab function `quad2d`.

Case #4: $N_0 > 0$, α_{00} and α_{01} are statistically independent, τ -delay is random.

Obviously, this is the most interesting case because, in practical applications, the value of τ is not known a priori. The model used in [1] assumes that τ is sampled from an exponential distribution (with parameter λ), but was pointed out in the same reference that τ should be rather modelled as a discrete random variable than as a continuous one. We introduce a new model for τ , which is discrete. The novel model is described by resorting to the following algorithm:

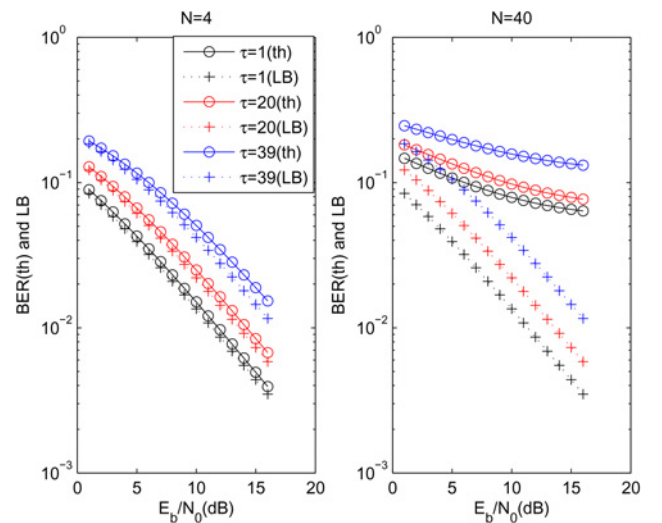


Fig. 1 Values of $\text{BER}(\text{th})$ obtained when computing numerically the integral in (18) are compared with LB – the lower bound in (25). These results are for $N=4$ users (left panel) and $N=40$ users (right panel). The values of the time delay τ are given in the legend. In addition, $s = 40$, $\beta = 50$ and $r_0 = 1.1$.

Step₀: Let $\tau_c \sim \text{Exponential}(\lambda)$, $\lambda > 0$. Hence, the PDF of τ_c is given by $f(\tau_c) = \lambda \ell^{\tau_c}$, where $\ell = \exp(-\lambda)$ and $\tau_c \geq 0$.

Step₁: $\tau_q \stackrel{\text{def}}{=} \lfloor \tau_c \rfloor$, where $\lfloor \cdot \rfloor$ denotes the largest integer not greater than the real number in the argument. It is clear that $\Pr(\tau_q = i) = (1 - \ell)\ell^i$ for $i \in \{0, 1, 2, \dots\}$.

Step₂: Take $\tau = \tau_q \pmod s$. Simple calculations lead to

$$\Pr(\tau = j) = \frac{1 - \ell}{1 - \ell^s} \ell^j \quad \text{for all } j \in \{0, 1, \dots, s-1\}. \quad (28)$$

Remark that τ cannot be equal to s . The model we introduced for τ leads to the following expression for BER

$$\text{BER} = \sum_{j=0}^{s-1} \Pr(\tau = j) \text{BER}(j), \quad (29)$$

where $\Pr(\tau = j)$ is given in (28) and $\text{BER}(j)$ is evaluated by using (26) and (27).

Remarks: It is clear that $E[\tau]$ and $E[\tau^2]$ are two important quantities involved in the evaluation of (29). This is why, we give below their expressions

$$E[\tau] = \frac{\ell}{1 - \ell^s} \frac{(s-1)\ell^s - s\ell^{s-1} + 1}{1 - \ell}, \quad (30)$$

$$E[\tau^2] = E[\tau] + \frac{\ell^2}{1 - \ell^s} \left[\frac{2(1 - \ell^s)}{(1 - \ell)^2} - \frac{2\ell^{s-1}s}{1 - \ell} - \ell^{s-2}s(s-1) \right]. \quad (31)$$

Proofs of the identities outlined above can be found in [21, Section 1.2.3]. At the same time, it is well-known that the moments of τ_c are

[22, Chapter 14]

$$E[\tau_c] = \frac{1}{\lambda}, \quad (32)$$

$$E[\tau_c^2] = \frac{2}{\lambda^2}. \quad (33)$$

In [21, Fig. 1.2], we compare the moments computed with (30) and (31) with those given by (32) and (33) for the case when $s = 40$ and $1/\lambda \in \{1, 2, \dots, 20\}$. In that figure, one can see that the moments of τ and τ_c are almost the same when the mean of τ_c is small, but they tend to be different when the mean of τ_c increases.

Following, we focus on the computation of BER when z in (4) is assumed to be Gaussian distributed.

4 Computation of BER by using the Gaussian approximation for z

For sake of comparison, we compute approximate BER's by applying the method from [1], which assumes the distribution of z to be Gaussian. We write down the calculations for the four cases considered in Section 3.3.

Case #1: The approximate BER, which we denote $\text{BER}(\tau)|_{E_b/N_0=\infty}$, is given by

$$\tilde{\text{BER}}(\tau)|_{E_b/N_0=\infty} = \frac{1}{2} \text{erfc}\left(\frac{\hat{\zeta}_\tau^{-1/2}}{\tau}\right), \quad (34)$$

where

$$\frac{\hat{\zeta}_\tau}{\tau} = \frac{2\text{Var}[z]}{(E[z])^2} = \frac{2E[z^2]}{(E[z])^2} - 2. \quad (35)$$

As $C = 0$, we employ (4), (7), (8) and [21, Lemma 3.2.2 Lemma 3.2.4] for the following calculations

$$E[z] = \{E[\alpha_{00}]s + E[\alpha_{01}](s - \tau)\}E[A] + E[\alpha_{01}]\tau E[B] \quad (36)$$

$$\begin{aligned} &= (\pi/2)^{1/2} [bs + \tilde{b}(s - \tau)]\beta, \\ E[z^2] &= \{s^2 E[\alpha_{00}^2] + (s - \tau)^2 E[\alpha_{01}^2] \\ &\quad + 2s(s - \tau)E[\alpha_{00}]E[\alpha_{01}]\}E[A^2] + \tau^2 E[\alpha_{01}^2]E[B^2] \\ &\quad + 2\tau\{sE[\alpha_{00}]E[\alpha_{01}] + (s - \tau)E[\alpha_{01}^2]\}E[AB] \end{aligned} \quad (37)$$

$$\begin{aligned} &= [2\tilde{b}^2(s - \tau)^2 + 2b^2s^2 + \pi b\tilde{b}s(s - \tau)] \\ &\quad \times [(N\beta)/2 - \beta/4 + \beta^2] \\ &\quad + 2\tau(\beta/4 - 1/4) \times [2\tilde{b}^2(s - \tau) + (b\tilde{b}s\pi)/2] + N\beta\tilde{b}^2\tau^2. \end{aligned} \quad (38)$$

Case #2: Using the notation from Section 3.3, we re-write the expression of z as $z = \alpha_{00}[s + (s - \tau)/r_0]A + \alpha_{00}(\tau/r_0)B + sC$. This leads to the following results

$$\begin{aligned} E[z] &= E[\alpha_{00}][s + (s - \tau)/r_0]E[A] \\ &= (\pi/2)^{1/2} b[s + (s - \tau)/r_0]\beta, \\ E[z^2] &= E[\alpha_{00}^2][s + (s - \tau)/r_0]^2 E[A^2] \\ &\quad + E[\alpha_{00}^2](\tau/r_0)^2 E[B^2] + s^2 E[C^2] \\ &\quad + 2E[\alpha_{00}^2][s + (s - \tau)/r_0](\tau/r_0)E[AB]. \end{aligned}$$

All that remains is to plug-in the expressions for the moments of the

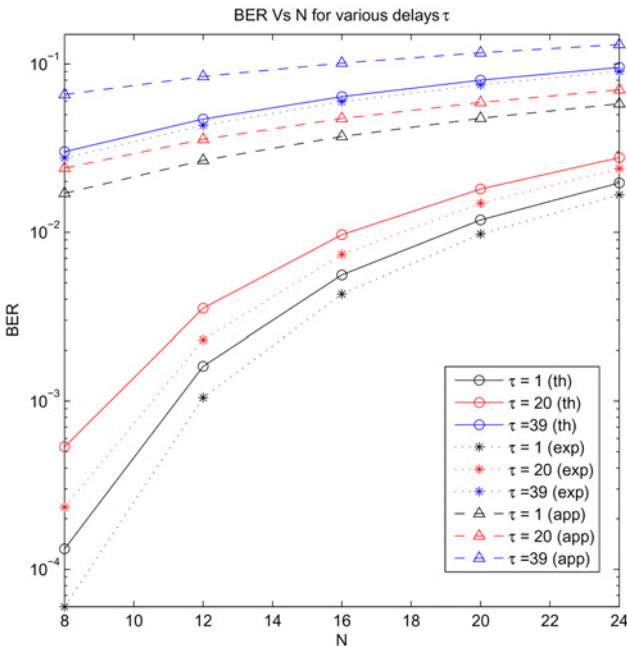


Fig. 2 Case #1: $\text{BER}(\text{exp})$ [computed empirically from 10^6 simulated bits] is compared with $\text{BER}(\text{th})$ [calculated by numerical integration with formulae from Section 3.3] and $\text{BER}(\text{app})$ [calculated with the Gaussian approximation from Section 4] when the number of users N increases from 8 to 24. Other settings: $\beta = 50$, $b = \sqrt{2}/2$, $\tilde{b} = 0.9b$ and the values of τ are listed in the legend of the figure

random variables involved, to calculate ξ like in (35) and then to use the $\text{erfc}(\cdot)$ function for computing $\text{BER}(\tau)|_{r=r_0}$.

Case #3: It is easy to see that, in this case, the expression of $E[z]$ coincides with the one in (36). Similarly, $E[z^2]$ can be calculated as the summation of (37) and (38) with $s^2 E[C^2]$. Note that $s^2 E[C^2] = s^2 N_0 \beta$ (see [21, Lemma 3.3.1]).

Case #4: It is straightforward to write down the following identities:

$$\begin{aligned} E[z] &= E[\delta_0]E[A], \\ E[\delta_0] &= -E[\tau]E[\alpha_{01}] + s\{E[\alpha_{00}] + E[\alpha_{01}]\}, \\ E[z^2] &= E[\delta_0^2]E[A^2] + E[\delta_1^2]E[B^2] + s^2 E[C^2] + 2E[\delta_0 \delta_1]E[AB], \\ E[\delta_0^2] &= E[\tau^2]E[\alpha_{01}^2] - 2sE[\tau]\{E[\alpha_{01}^2] + E[\alpha_{00}]E[\alpha_{01}]\} \\ &\quad + s^2\{E[\alpha_{00}^2] + E[\alpha_{01}^2] + 2E[\alpha_{00}]E[\alpha_{01}]\}, \\ E[\delta_1^2] &= E[\tau^2]E[\alpha_{01}^2], \\ E[\delta_0 \delta_1] &= -E[\tau^2]E[\alpha_{01}^2] + E[\tau]s\{E[\alpha_{00}]E[\alpha_{01}] + E[\alpha_{01}^2]\}. \end{aligned}$$

The moments of z can be then evaluated with the help of results from [21, Lemma 3.2.2, Lemma 3.2.4 Lemma 3.3.1] and (7), (8). For the first- and second-order moments of τ we apply (30) and (31).

Following, we resort to numerical examples for a better understanding of the results obtained so far.

5 Numerical examples

5.1 Experimental settings

In this section, we compare the theoretical BER with the empirical values obtained from simulations. All the results are plotted in [21, Figs. 2.1–2.8]. Due to the limited space, we display here only some of these figures. We mention that each experimental result shown in [21, Figs. 2.1–2.8] is produced by simulating the transmission of

10^6 bits. In all cases, the spread factor is $2\beta = 100$ and each chip is extended into $s=40$ samples. The parameter b of the Rayleigh distribution from which we sample α_{00} is taken to be $\sqrt{2}/2$. This choice guarantees that the expected power of fading on the main channel is one: $E[\alpha_{00}^2] = 1$ [see (8)]. Selection of other parameters is explained below, for each considered case. The nomenclature for the four cases we analyse is the same as in Sections 3.3 and 4.

5.2 Experimental results

Case #1: In addition to $b = \sqrt{2}/2$, we set the parameter of the Rayleigh distribution for α_{01} to be $\tilde{b} = 0.9b$. As the additive Gaussian noise is not considered ($E_b/N_0 \rightarrow \infty$), we are mainly concerned with the degradation of performance when the number of users increases. This is why we plot BER versus N in Fig. 2. The values of BER are computed as follows (in parentheses we indicate the acronyms used in the legend of the figure): (th) numerical integration of (15); (app) Gaussian approximation in (34); and (exp) simulation of 10^6 bits. Remark in the same figure that $\tau \in \{1, s/2, s-1\}$, where $s=40$. Disregarding how BER is computed, BER increases when the ratio τ/s raises and N is kept fixed. We also remark that, for a given value of τ/s , BER grows when N becomes larger. These results are not surprising and they are in line with the analysis from Section 3. Remark the agreement between the values of BER(th) and BER(exp). However, for a given set of experimental parameters, BER(app) is much larger than both BER(th) and BER(exp), which shows clearly that in the absence of additive Gaussian noise, the Gaussian assumption for z leads to a poor approximation of BER.

Case #2: In contrast to Case #1, we now take E_b/N_0 to be relatively small, namely $E_b/N_0 = 2$ dB. Then we choose $r_0 = 1.1$ [see (16)] and keep all other settings as shown in Fig. 2. The theoretical and empirical values of BER are shown in [21, Fig. 2.2]. Observe the nearly linear dependence between BER and the number of users.

In the second experiment conducted for Case #2, we maintain all the settings as in the first one, except that $N=4$ and E_b/N_0 is varied between 1 and 8 dB. The results are plotted in [21, Fig. 2.3], where

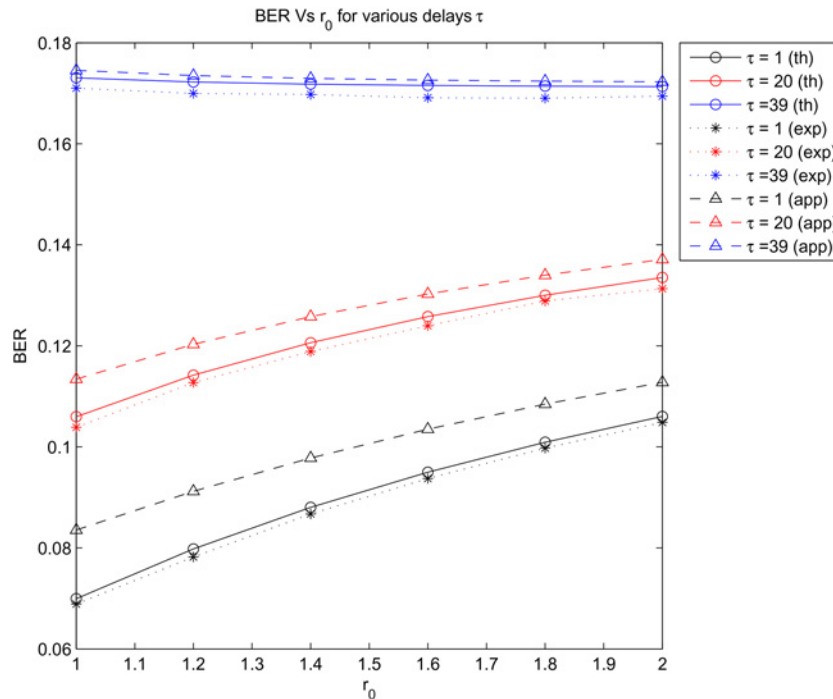


Fig. 3 Case #2: In order to investigate the impact of r_0 on the performance of the CDMA-system, we alter the settings such that $N=4$, $E_b/N_0 = 2$ dB and $r_0 \in \{1, 1.2, \dots, 2\}$. For clarity of the representation, we prefer to use for ordinates the linear scale instead of the logarithmic scale

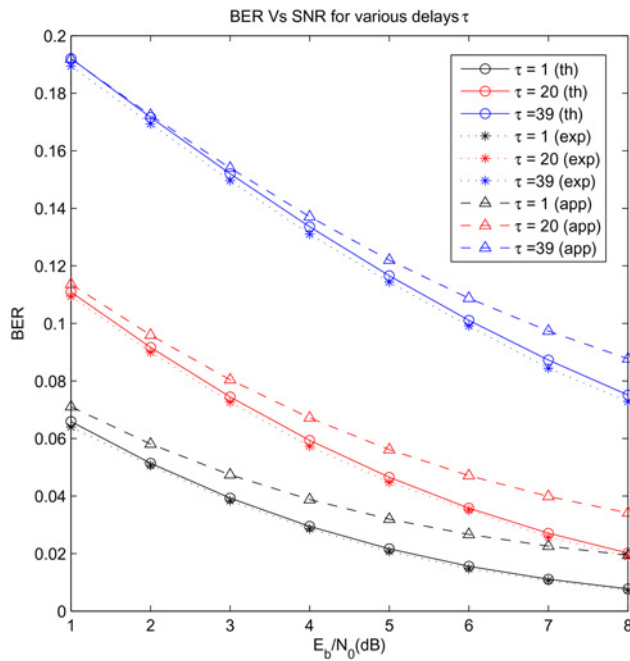


Fig. 4 Case #3 The number of users is $N = 4$ and the variance of the additive Gaussian noise (N_0) is varied in order to see the effect of E_b/N_0 on BER (th) [see Section 3.3], BER(app) [see Section 4] and BER(exp) [computed empirically]. All other settings are the same as in Fig. 2

we can see the improvement in performance when E_b/N_0 grows. In the same figure can be also observed how inaccurate the Gaussian approximation is when E_b/N_0 is relatively large. For instance, the

BER computed with Gaussian approximation when $\tau = 1$ and $E_b/N_0 = 8$ dB is not only larger than the empirical BER obtained for the same experimental settings, but is also larger than the empirical BER corresponding to $\tau = 20$ and $E_b/N_0 = 8$ dB.

In the last experiment for Case #2, the focus is on r_0 . We fix $N = 4$, $E_b/N_0 = 2$ dB and let r_0 to take values from the set $\{1, 1.2, \dots, 2\}$. According to Fig. 3, the increase of r_0 slightly lowers the BER if $\tau = s - 1$. On the contrary, BER is monotonically increasing with r_0 when $\tau \in \{1, s/2\}$. For understanding this behaviour, we use the definitions in Section 3.3 for evaluating $\zeta_{\alpha_{00}, \tau}$. For example, when $\tau = 39$, we have $s/\tau \simeq 1$, which implies $D_1 \simeq r_0$ and $D_2 \simeq 1$. It follows that:

$$\begin{aligned}\zeta_{\alpha_{00}, 39} &\simeq \frac{N}{r_0^2 \beta} + \frac{\beta - 1}{r_0 \beta^2} + \text{ct}(r_0) \\ &\simeq \frac{0.08}{r_0^2} + \frac{0.02}{r_0} + \text{ct}(r_0),\end{aligned}$$

where $N = 4$, $\beta = 50$ and $\text{ct}(r_0)$ represents those terms which do not depend on r_0 . Hence, if r_0 grows, then $\zeta_{\alpha_{00}, 39}$ becomes smaller and $\text{BER}(39)|_{r=r_0}$ decreases [see (18)]. For $\tau = 1$, we have $D_1 \simeq s(r_0 + 1)$ and $D_2 \simeq 1 + 1/r_0$. So

$$\begin{aligned}\zeta_{\alpha_{00}, 1} &\simeq \frac{N}{s^2(r_0 + 1)^2 \beta} + \frac{\beta - 1}{s(r_0 + 1) \beta^2} \\ &\quad + \frac{1}{(1 + 1/r_0)^2} \frac{1}{\alpha_{00}^2} \frac{2N_0}{\beta} + \text{ct}(r_0) \\ &\simeq \frac{5 \times 10^{-5}}{(r_0 + 1)^2} + \frac{5 \times 10^{-4}}{r_0 + 1} + \frac{1}{\alpha_{00}^2} \frac{1.26}{(1 + 1/r_0)^2} + \text{ct}(r_0).\end{aligned}$$

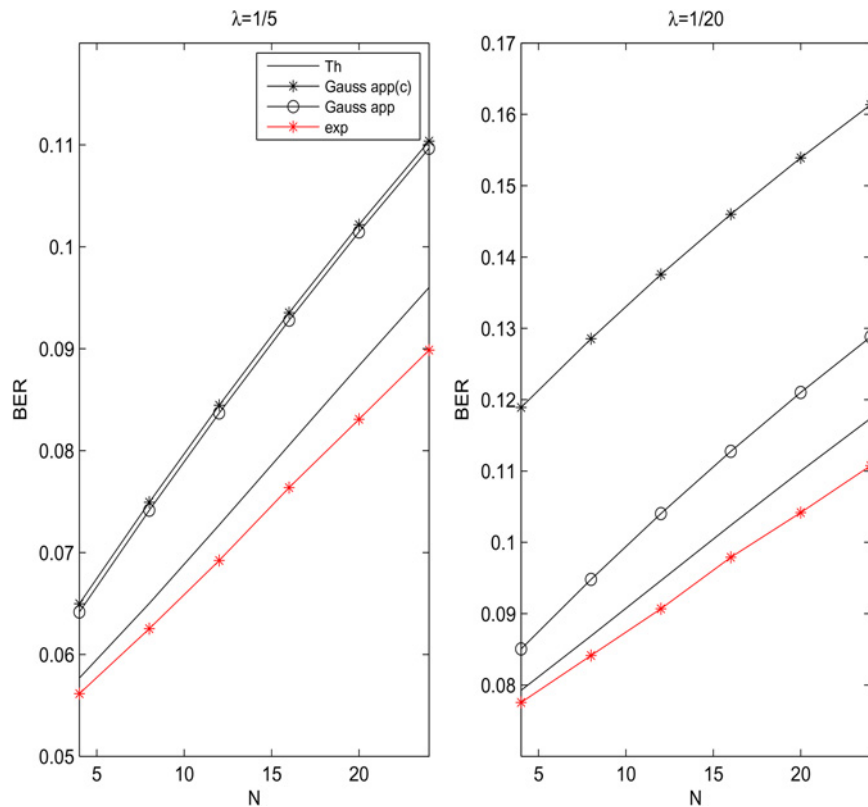


Fig. 5 Case #4: Comparison of BER(Th), which represents the BER given in (29), with two Gaussian approximations. The first approximation [Gauss app(c)] employs the formulae in (32) and (33), whereas the second one [Gauss app] uses (30) and (31). In addition, $b = \sqrt{2}/2$, $\bar{b} = 0.9b$, $2\beta = 100$, $s = 40$ and $E_b/N_0 = 2$ dB. The parameter of the exponential distribution from which τ_c is drawn is either $1/5$ (left panel) or $1/20$ (right panel). For each value of N (number of users) shown in the plots, BER(exp) is computed by simulating the transmission of 10^6 bits

As we know $E[\alpha_{00}^2] = 1$, it means that the dominant term in the equation above is the one that contains the factor $1/\alpha_{00}^2$. This leads to the conclusion that $\zeta_{\alpha_{00},1}$ is monotonically increasing with r_0 and explains the behaviour observed in Fig. 3.

Case #3: Similar to Case #1, we take $\tilde{b} = 0.9b$ for the plots in Fig. 4 and [21, Fig. 2.5]. In [21, Fig. 2.5], $E_b/N_0 = 2$ dB and the number of users ranges from 4 to 24. It is interesting that the difference between BER(th) and BER(exp) increases when N raises, but at least for $\tau = 1$ and $\tau = 20$, $\text{BER}(\text{th}) - \text{BER}(\text{exp})$ is clearly smaller than $\text{BER}(\text{app}) - \text{BER}(\text{exp})$.

In the particular case of Fig. 4, the number of users is small ($N = 4$) and we remark the decrease of BER when E_b is kept fixed and N_0 is lowered. As already observed in other graphs within this section, $\text{BER}(\text{th})$ and $\text{BER}(\text{exp})$ are almost the same. In addition, the Gaussian approximation $\text{BER}(\text{app})$ almost coincides with $\text{BER}(\text{th})$ when E_b/N_0 is small. The smaller N_0 is, the worse the Gaussian approximation is, and this trend confirms what we have already noticed for Case #1 and Case #2.

Another interesting aspect is that in Case #2, the ratio α_{00}/α_{01} is fixed to 1.1, while in Case #3 the ratio of the means of distributions from which α_{00} and α_{01} are drawn is about 1.1. This explains the similarities between figures [21, Fig. 2.2] and [21, Fig. 2.5] as well as the similarities between figures [21, Fig. 2.3] and [21, Fig. 2.6].

Case #4: The key point is the randomness of the delay τ . As we already know from Section 3.3, τ is a random variable obtained by quantising τ_c . Bearing in mind that, in our settings, the maximum possible value of τ is $s-1 = 39$, we conduct experiments for the situation when τ is sampled from an exponential

distribution with mean 5, as well as for the case when the mean of the exponential distribution is 20. All other experimental settings are described in Fig. 5, where we show how the BER depends on the number of users (N). We are mainly interested in comparing the theoretical BER given in (29) with the empirical results obtained from simulations. Under the assumption that z is Gaussian distributed, the approximate BER is calculated by using the expressions of $E[\tau]$ and $E[\tau^2]$ from (30) and (31) in the formulae outlined in Section 4. For comparison with results reported previously (see [1]), we also compute another approximate BER which is obtained by employing the formulae in (32) and (33) for $E[\tau]$ and $E[\tau^2]$, respectively. As we can see in Fig. 5, the two Gaussian approximations can differ significantly if $1/\lambda$ (the mean of the exponential distribution from which τ_c is sampled) is large. In the same figure, one can observe the difference between BER computed with (29) and the Gaussian approximations. The fact that the two Gaussian approximations are over-pessimistic can be also observed in Fig. 6, where the number of users is fixed and the ratio E_b/N_0 is increased from 1 to 8 dB.

With the exception of Fig. 2, a common characteristic of the plots within this section is the relatively low value of the E_b/N_0 -ratio used in simulations. In spite of the fact that the performance of the CDMA system is modest, we preferred to use low values for E_b/N_0 because they correspond to the situation when the Gaussian approximation for z [see (4)] is still reasonably well. When the variance of additive noise is decreased, the gap between BER computed with the approximation in [1] and the empirical results becomes larger.

All the experimental results reported in this work can be reproduced by using our Matlab implementation which can be

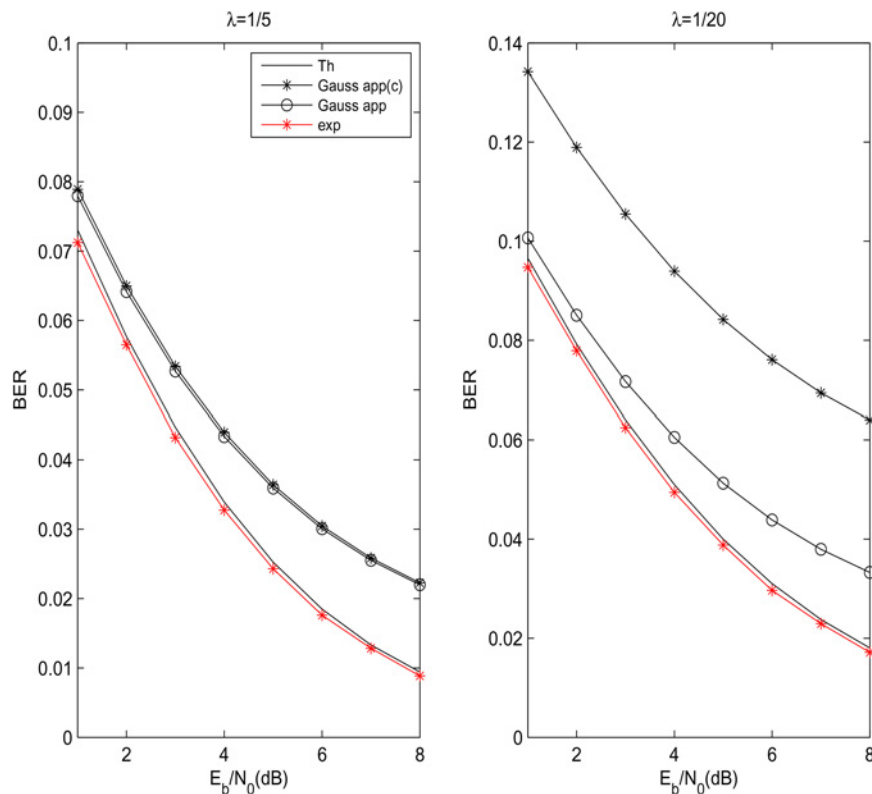


Fig. 6 Case #4: For this figure, all settings are the same as in Fig. 5, except that the number of users is fixed to $N = 4$ and the variance of the additive Gaussian noise N_0 is selected such that E_b/N_0 takes the values shown on the abscissas of the plots

6 Final remarks

We demonstrated that the approximations applied in [1] for computing the BER of chaos-based CDMA systems in wide-band channels lead to over-pessimistic results when the number of secondary paths is small, and we proposed a novel methodology for computing more accurately the BER. In our derivations, we have used a number of supplementary assumptions. For instance, we have assumed that all the transmitted bits have value ‘+1’ (see Table 1). However, we provide in [21, Section 1.2.4 and Section 3.5] a rigorous proof of the fact that BER remains the same, disregarding the values of the bits transmitted for all N users.

All our calculations were performed for the case when the logistic map is employed. The results can be extended to other chaotic maps because the computation of the conditional BER relies only on the first- and second-order moments, and these are already known for the chaotic maps (see, e.g. [2]). The problems occur when BER is evaluated by using the conditional BER because all the integrals involved depend on the channel model. We have only considered the Rayleigh model. For other models, the calculations might be more difficult (see, e.g. [26]).

7 Acknowledgments

The research activity of C.D. Giurcăneanu at University of Auckland (New Zealand) was supported by the Project no. 3702543 (Science FRDF New Staff).

8 References

- [1] Berber S.: ‘Probability of error derivatives for binary and chaos-based CDMA-systems in wide-band channels’, *IEEE Trans. Wirel. Commun.*, 2014, **13**, (10), pp. 5596–5606
- [2] Lau F.C.M., Tse C.K.: ‘Chaos-based digital communication systems. Operating principles, analysis methods, and performance evaluation’ (Springer, 2003)
- [3] Lawrance A.: ‘Statistical aspects of chaotic maps with negative dependence in communications setting’, *J. R. Stat. Soc. B*, 2001, **63**, (Part 4), pp. 843–853
- [4] Geisel T., Failen V.: ‘Statistical properties of chaos in Chebyshev maps’, *Phys. Lett.*, 1984, **105A**, (6), pp. 263–266
- [5] Lawrance A., Ohama G.: ‘Exact calculation of bit error rates in communication systems with chaotic modulation’, *IEEE Trans. Circuits Syst., Fundam. Theory Appl.*, 2003, **50**, (11), pp. 1391–1400
- [6] Kaddoum G., Lambard T., Gagnon F.: ‘Performance analysis of a chaos shift keying system with polarisation sensitivity under multipath channel’, *IET Commun.*, 2012, **6**, (12), pp. 1837–1845
- [7] Kaddoum G., Gagnon F.: ‘Lower bound on the bit error rate of a decode-and-forward relay network under chaos shift keying communication system’, *IET Commun.*, 2014, **8**, (2), pp. 227–232
- [8] Kaddoum G., Gagnon F.: ‘Design of a high-data-rate differential chaos-shift keying system’, *IEEE Trans. Circuits Syst., Express Briefs*, 2012, **59**, (7), pp. 448–452
- [9] Yang H., Jiang G.-P.: ‘High-efficiency differential-chaos-shift-keying scheme for chaos-based noncoherent communication’, *IEEE Trans. Circuits Syst., Express Briefs*, 2012, **59**, (5), pp. 312–316
- [10] Yang H., Jiang G.-P.: ‘Reference-modulated DCSK: a novel chaotic communication scheme’, *IEEE Trans. Circuits Syst., Express Briefs*, 2013, **60**, (4), pp. 232–236
- [11] Yang H., Jiang G.-P., Duan J.: ‘Phase-separated DCSK: a simple delay-component-free solution for chaotic communications’, *IEEE Trans. Circuits Syst., Express Briefs*, 2014, **61**, (12), pp. 967–971
- [12] Sushchik M., Tsimring L., Volkovskii A.: ‘Performance analysis of correlation-based communication schemes utilizing chaos’, *IEEE Trans. Circuits Syst., Fundam. Theory Appl.*, 2000, **47**, (12), pp. 1684–1690
- [13] Tam W., Lau F., Tse C., Lawrance A.: ‘Exact analytical bit error rates for multiple access chaos-based communication systems’, *IEEE Trans. Circuits Syst., Express Briefs*, 2004, **51**, (9), pp. 473–481
- [14] Kaddoum G., Charge P., Roviras D.: ‘A generalized methodology for bit-error-rate prediction in correlation-based communication schemes using chaos’, *IEEE Commun. Lett.*, 2009, **13**, (8), pp. 567–569
- [15] Kaddoum G., Coulon M., Roviras D., Charge P.: ‘Theoretical performance for asynchronous multi-user chaos-based communication systems on fading channels’, *Signal Process.*, 2010, **90**, pp. 2923–2933
- [16] Vali R., Berber S., Nguang S.: ‘Analysis of chaos-based code tracking using chaotic correlation statistics’, *IEEE Trans. Circuits Syst., Fundam. Theory Appl.*, 2012, **59**, (4), pp. 796–805
- [17] Vali R., Berber S., Nguang S.: ‘Accurate performance analysis of chaos-based code tracking in presence of multipath fading’, *Electron. Lett.*, 2012, **48**, (4), pp. 238–240
- [18] Saleh A., Valenzuela R.: ‘A statistical model for indoor multipath propagation’, *IEEE J. Sel. Areas Commun.*, 1987, **SAC-5**, (2), pp. 128–137
- [19] Andreas F.M., Kannan B., Dajana C., ET AL.: ‘IEEE 802.15.4a channel model’. Final report, London, UK, 2005
- [20] Xia Y., Tse C.K., Lau F.C.M.: ‘Performance of differential chaos-shift-keying digital communication systems over a multipath fading channel with delay spread’, *IEEE Trans. Circuits Syst., Express Briefs*, 2004, **51**, (12), pp. 680–684
- [21] Giurcăneanu C., Abeywickrama R., Berber S.: ‘Supplemental material to: ‘Performance analysis for a chaos-based CDMA system in wide-band channel’’, <https://www.stat.auckland.ac.nz/cgiui216/PUBLICATIONS.htm>, 2015
- [22] Evans M., Hastings N., Peacock B.: ‘Statistical distributions’ (John Wiley & Sons, 2000)
- [23] Kendall M., Stuart A.: ‘The advanced theory of statistics, Vol. I: Distribution theory’ (Charles Griffin & Company Limited, 1977)
- [24] Chernov N.: ‘Limit theorems and Markov approximations for chaotic dynamical systems’, *Probab. Theory Relat. Fields*, 1995, **101**, pp. 321–362
- [25] Khoolejani N.B., Khorshidian K.: ‘On the ratio of Rice random variables’, *J. Iran. Stat. Soc.*, 2009, **8**, (1–2), pp. 61–71
- [26] Simon M.K., Alouini M.-S.: ‘Digital communication over fading channels’ (John Wiley & Sons, 2005)

9 Appendix

9.1 Proof of Proposition 1

It is enough to observe in (21) that $v > 0$, which leads to

$$\begin{aligned}
 \text{BER}(\tau)|_{r=r_0} &\geq \frac{1}{2} \int_0^\infty \text{erfc}(\sqrt{\gamma/w}) f(\gamma) d\gamma \\
 &= \int_0^\infty Q(\sqrt{2\gamma/w}) f(\gamma) d\gamma \\
 &= \frac{1}{\pi} \int_0^\infty \left[\int_0^{\pi/2} \exp\left(-\frac{\gamma/w}{\sin^2 \theta}\right) d\theta \right] f(\gamma) d\gamma \\
 &= \frac{1}{\pi} \int_0^{\pi/2} \left[\int_0^\infty \exp\left(-\frac{\gamma/w}{\sin^2 \theta}\right) \frac{\exp(-\gamma/\bar{\gamma})}{\bar{\gamma}} d\gamma \right] d\theta \\
 &= \frac{1}{\pi} \int_0^{\pi/2} \left(1 + \frac{\bar{\gamma}}{w \sin^2 \theta} \right)^{-1} d\theta
 \end{aligned} \tag{39}$$

$$= \frac{1}{2} \left(1 - \frac{1}{\sqrt{1 + w/\bar{\gamma}}} \right). \tag{40}$$

In (39), we applied the identity from [26, Eq. (5.3)], while in (40) we employed [26, Eq. (5.6)].